Biochimica et Biophysica Acta 1818 (2012) 627–635

Contents lists available at SciVerse ScienceDirect

Biochimica et Biophysica Acta

journal homepage: www.elsevier.com/locate/bbamem

Acyrthosiphon pisum AQP2: A multifunctional insect aquaglyceroporin

Ian S. Wallace [a,1], Ally J. Shakesby [b], Jin Ha Hwang [a], Won Gyu Choi [a], Natália Martínková [b,c], Angela E. Douglas [b,d], Daniel M. Roberts [a,*]

[a] Department of Biochemistry & Cellular, and Molecular Biology, The University of Tennessee, Knoxville, Knoxville, TN, 37996–0840, USA
[b] Department of Biology, University of York, York, YO10 5DD, UK
[c] Institute of Vertebrate Biology, Academy of Sciences of the Czech Republic, v.v.i., Květná 8, 603 65 Brno, Czech Republic
[d] Department of Entomology, Comstock Hall, Cornell University, Ithaca, NY 14850, USA

ARTICLE INFO

Article history:
Received 31 August 2011
Received in revised form 19 November 2011
Accepted 28 November 2011
Available online 8 December 2011

Keywords:
Aphid
Aquaporins
Buchnera aphidicola
Osmoregulation
Polyols
Symbiosis

ABSTRACT

Annotation of the recently sequenced genome of the pea aphid (*Acyrthosiphon pisum*) identified a gene *ApAQP2* (ACYPI009194, Gene ID: 100168499) with homology to the Major Intrinsic Protein/aquaporin superfamily of membrane channel proteins. Phylogenetic analysis suggests that ApAQP2 is a member of an insect-specific clade of this superfamily. Homology model structures of ApAQP2 showed a novel array of amino acids comprising the substrate selectivity-determining "aromatic/arginine" region of the putative transport pore. Subsequent characterization of the transport properties of ApAQP2 upon expression in *Xenopus* oocytes supports an unusual substrate selectivity profile. Water permeability analyses show that the ApAQP2 protein exhibits a robust mercury-insensitive aquaporin activity. However unlike the water-specific ApAQP1 protein, ApAQP2 forms a multifunctional transport channel that shows a wide permeability profile to a range of linear polyols, including the potentially biologically relevant substrates glycerol, mannitol and sorbitol. Gene expression analysis indicates that ApAQP2 is highly expressed in the insect bacteriocytes (cells bearing the symbiotic bacteria *Buchnera*) and the fat body. Overall the results demonstrate that ApAQP2 is a novel insect aquaglyceroporin which may be involved in water and polyol transport in support of the *Buchnera* symbiosis and aphid osmoregulation.

1. Introduction

Major Intrinsic Proteins (MIPs) are an ancient class of integral membrane protein channels that facilitate the selective bidirectional transport of water and uncharged solutes across biological membranes [1]. The aquaporins represent the best characterized transporters in this family, and these proteins play diverse roles in physiology by mediating the bulk movement of water driven by osmotic and pressure gradients [1–3]. Members of the MIP superfamily share a signature topology and pore architecture, referred to as the "hourglass fold". This topology consists of six transmembrane α-helices related by a pseudo two-fold symmetry [4]. Additionally, two highly conserved loops between transmembrane α-helices 2 and 3, and transmembrane α-helices 5 and 6 form two smaller α-helical segments (the "NPA" boxes) which fold back into the protein and pack with the six transmembrane α-helices, forming a 7th pseudo transmembrane helix [4]. The pore formed by the packing of these helices resembles an hourglass with the transport selectivity determined by a narrow constriction, the "aromatic/arginine" (ar/R) selectivity filter [4,5]. The ar/R selectivity filter is defined by four residues (one each from transmembrane helices 2 and 5, and two from the interhelical loop containing the second NPA box) that mediate transport selectivity based on solute size and hydrophobicity. Vertebrate MIPs generally fall into two broad transport classes, water-selective aquaporins and multifunctional aquaglyceroporins that differ in the amino acid composition of the ar/R [3].

While the transport behavior and physiology of vertebrate aquaporins have been the subject of intensive study [3], the structure, function, and physiology of invertebrate MIPs are less well studied [2]. In the case of insects (e.g. bed bugs, mosquitoes, aphids, plant hoppers) that ingest large volumes of vertebrate blood or plant sap, aquaporins have been implicated in the bulk water movement across various cellular membranes in the gut, participating in volume and osmotic homeostasis, and fluid excretion [2,6–9]. For example, a water-selective aquaporin, ApAQP1, expressed in both the stomach and closely juxtaposed distal intestine of the plant-sap feeding pea aphid (*Acyrthosiphon pisum*) has been proposed to serve an osmoregulatory role in water cycling [9].

Analysis of the recently sequenced genome of *A. pisum* [10] revealed the presence of a second MIP gene encoding an aquaporin-like protein (ApAQP2) that is represented among ESTs obtained from both whole aphids [11] and isolated bacteriocytes [12]. Bacteriocytes are specialized aphid cells that house and maintain intracellular symbiotic γ-

* Corresponding author. Tel.: +1 865 974 4070; fax: +1 865 974 6306.
E-mail address: drobert2@utk.edu (D.M. Roberts).
[1] Present address: The Energy Biosciences Institute, 130 Calvin lab MC5230, Berkeley, CA, 94720, USA.

0005-2736/$ – see front matter © 2011 Elsevier B.V. All rights reserved.
doi:10.1016/j.bbamem.2011.11.032

proteobacteria *Buchnera aphidicola* (reviewed in [13]). The symbiosis has a nutritional basis: *Buchnera* provide the insect with essential amino acids that are in short supply in the aphid diet of plant phloem sap [14,15]. In this study, molecular modeling and functional analysis reveal that ApAQP2 is a multifunctional aquaglyceroporin channel that shows unique ar/R pore structure and exhibits permeability to a wide range of physiologically relevant polyols and is localized to both bacteriocytes and the fat body (an insect organ that functions in energy storage and immunity). The potential significance of this second aquaporin channel for the physiology of the insect, including its symbiosis with intracellular bacteria, is discussed.

2. Materials and methods

2.1. ApAQP2 cDNA cloning

Acyrthosiphon pisum clone LL01 was maintained on broad bean *Vicia faba* cv. The Sutton, grown at 20 °C with a 16 h light/8 h dark cycle. Aphids were homogenized in ice-cold TRIzol reagent (Invitrogen) and RNA was extracted following manufacturer's instructions (Invitrogen). To remove contaminating DNA, the RNA was incubated with RNAse-free DNAseI (Roche) for 30 min at 37 °C then at 75 °C for 15 min before purification with the RNAeasy minikit (Qiagen) using the RNA cleanup protocol.

For *ApAQP2* cDNA cloning, first strand cDNA was synthesized from RNA using Superscript II reverse transcriptase (Invitrogen) following the manufacturer's instructions. *ApAQP2* was amplified in 1× PCR buffer, 1 mM $MgSO_4$, 0.2 mM of each dNTP, 1 U KOD Hot Start Polymerase (Toyobo), 2 μL template (ca. 0.5 μg) and 1 μM gene-specific primers (Supplemental Table 1) with the following conditions: 31 cycles of 94 °C for 1 min, 35 °C for 1 min, and 72 °C for 2 min 30 s. PCR products were purified by electrophoresis in a 1% (w/v) agarose gel and were cloned into the pCR®-Blunt II-TOPO® plasmid vector (Invitrogen) following the manufacturer's instructions. Cloned PCR products were identified as *ApAQP2* by sequencing using an Applied Biosystems 3130 Genetic Analyzer (University of York Technology Facility, York, U.K.).

2.2. Real time Q-PCR analysis of ApAQP2 transcript abundance

Embryo, fat body, gut, bacteriocyte and head tissues were dissected from 7-day-old final instar larvae using fine pins and scissors, and the RNA was extracted from these tissues and parallel samples of whole aphids, as described earlier. cDNAs were generated from isolated RNA samples using Superscript II reverse transcriptase (Invitrogen) and $p(dN_6)$ random hexamers (Roche). Control reactions without reverse transcriptase (−RTase) were included in all assays. The abundance of *ApAQP2* transcripts was determined by Q-PCR with an ABI Prism 7900 Sequence Detection System (Applied Biosystems), using the comparative Ct method. The reaction mixtures contained 1× Power SYBR Green MasterMix (Applied Biosystems), 0.1 μM gene-specific primers (Supplemental Table 1), and 2 μL cDNA template in a final reaction volume of 25 μL. Thermal cycling conditions were 2 min at 50 °C, 10 min at 95 °C followed by 40 cycles of 15 s at 95 °C and 1 min at 60 °C. The assays included a dissociation curve (95 °C for 30 s followed by a 60–95 C temperature ramp in increments of 0.5 °C for 1 min each), which confirmed that all detectable fluorescence was derived from specific products. All experimental samples were assayed in triplicate, with template free and -RTase controls. The relative expression of ApAQP2 was assessed by determining the threshold cycle (Ct), and each transcript was normalized to the expression of the ribosomal protein L32 transcript (*RPL32*) standardized to the expression level of the transcript in the whole aphid body.

2.3. Expression and functional analyses of ApAQP2 in Xenopus laevis oocytes

The *ApAQP2* open reading frame (ORF) was amplified by PCR from the pCR Blunt-II TOPO vector (Invitrogen) with ExTaq polymerase and gene-specific primers (Supplemental Table 1) containing *Bam*HI restriction sites, and was cloned into the *Bgl*II site of the pXβG-FLAG vector by the approach described in [16]. The final expression construct contained *ApAQP2* open reading frame translationally fused to an N-terminal FLAG epitope tag.

Capped cRNA was produced from *Xba*I-linearized Flag-*ApAQP2*/pXβG and soybean *nodulin 26*/pXβG constructs by using the AmpliCap-Max T3 High Yield Message Maker Kit (Epicentre Technologies). Stage V and VI *X. laevis* oocytes were microinjected and cultured as described previously [9,16]. Experimental oocytes were injected with 46 nL of 1 ng/nL of each test cRNA, and negative control oocytes were injected with an equivalent volume of sterile RNase-free water. Expression of ApAQP2 and nodulin 26 proteins in oocytes was quantified by Western blot analysis of oocyte lysates using an anti-FLAG epitope monoclonal antibody (Stratagene) for ApAQP2-injected oocytes, and an antibody against soybean nodulin 26 for nodulin 26-injected oocytes as previously described [16–18]. The osmotic water permeability (P_f) of *Xenopus* oocytes was determined as previously described [16,18]. Oocytes were placed in a 15 °C bath solution containing diluted (30%) frog Ringers solution [16–18], and serial images of the oocytes were collected as they began to swell in response to hypoosmotic challenge. The rate of oocyte swelling ($d[V/V_0]/dt$) determined by video microscopy was used to calculate the osmotic permeability coefficient (P_f) using the following equation:

$$P_f = \frac{V_0/S_0(d[V/V_0]/dt)}{\left(\frac{S_{real}}{S_{sphere}}\right)V_w(\mathrm{osm}_{in}-\mathrm{osm}_{out})}$$

where V_0 is the initial volume and S_o is the initial surface area of the oocyte, osm_{in} is the osmolarity on the inside of the oocyte, osm_{out} is the osmolarity of the bathing solution, V_w is the partial molar volume of water (18 cm^3/mol), S_{real} is the actual oocyte surface area, and S_{sphere} is the theoretical oocyte surface area assuming a perfect sphere. A value of S_{real}/S_{sphere} of 9 was used in all calculations to correct for the increase in oocyte plasma membrane area resulting from the presence of folds and microvilli [18].

The effect of mercurials on transport was investigated by preincubating *ApAQP2*-injected oocytes in frog Ringers solution supplemented with 1 mM $HgCl_2$ for 5 min prior to assay. The viability of control and ApAQP2-expressing oocytes was verified by measurement of the resting oolemma membrane potentials as described in [19]. All oocytes possessed inwardly negative resting potentials between −22 and −25 mV, consistent with the reported membrane potential values of viable oocytes [20].

Xenopus oocytes expressing ApAQP2 were assayed for solute permeability by two different methods. Nonradiolabeled solute uptake assays were performed by measuring solute-induced swelling under isoosmotic conditions as previously described [16]. The oocytes were placed into a bath solution containing isoosmotic frog Ringers solution with the NaCl component replaced with 200 mM test solute. In this assay, solute uptake results in an inwardly-directed osmotic gradient that leads to water uptake and oocyte swelling. Solute uptake is reported as an oocyte swelling rate [$d(V/V_0)/dt$], determined by video microscopy.

Radiolabeled glycerol and mannitol uptake assays were performed by a method modified from [16]. Twelve oocytes were incubated in 150 μL of 5 mM HEPES NaOH pH 7.6, 86 mM NaCl, 2 mM KCl, 5 mM $MgCl_2$, 0.6 mM $CaCl_2$ supplemented with 20 mM ^{3}H-glycerol (14 μCi/mL) for glycerol uptake assays, or with 20 mM ^{14}C-mannitol (1.4 μCi/mL) for mannitol uptake assays. All radioisotopic assays were conducted for 10 min at 25 °C. The oocytes were rinsed four times

with 10 mL of radioisotope-free, ice-cold assay buffer, and separated into three groups of four oocytes in scintillation vials. The oocytes were lysed in 300 μL of 10% (w/v) SDS and isotope uptake was quantified by as in [16].

2.4. Molecular modeling

A homology model of ApAQP2 was constructed using the Molecular Operating Environment software (MOE2009.10; Chemical Computing Group, Montreal, Canada). The crystal structure of human AQP4 (pdb 3GD8 [21]) was chosen as the structural template because of its high resolution (1.8 Å) and the high level of amino acid sequence identity (33%) to the ApAQP2 amino acid sequence within transmembrane helical regions that form the transport pore. Similar results were obtained with other aquaporin structural templates (data not shown). ApAQP2 was aligned with the AQP4 template by using the MOE structural alignment tool. Homology models were constructed by using the homology modeling facility in MOE and the CHARMM27 force field. An ensemble of ten possible structures for ApAQP2 was generated and ranked by packing score. The model with the most favorable packing score (3.0373) was energy-minimized using the CHARMM27 force field and distance-dependent dielectric down to an energy gradient of 10^{-5} kcal/mol/Å^2. The stereochemical quality of the final model was assessed by using Ramachandran plot analysis and the Protein Report structural analysis function in the MOE Protein Structure Evaluation package as previously described [22] to determine disallowed bond angles, bond lengths, and side-chain rotamers. The final ApAQP2 model possessed two residue outliers in the Ramachandran plot. Both residues were found in the unconserved and unstructured region of the C loop which does not contribute to the formation of the aquaporin fold and transport pore. Pore diameters of homology models were calculated using the HOLE2.0 program [23] of the energy minimized homology model structure using the simple.rad van der Waals radius file.

2.5. Phylogenetic analysis

The protein sequences were aligned using ClustalX [24], checked manually in BioEdit 5.0.9 [25] and truncated to remove the predicted N and C terminal cytoplasmic tails, which could not be aligned with confidence. Bayesian inference (BI) and maximum likelihood (ML) analyses were conducted, following selection of the WAG + Γ + I model [26], using the optimal instantaneous rate matrix estimated in ProtTest 1.4 [27]. The gamma shape parameter α and proportion of invariable sites were estimated as part of the analysis. Eight rate categories were used for rate heterogeneity estimation. The BI analysis was run in MrBayes 3.1.2 [28]. Data were processed in two partitions. In the first partition, gaps in the amino-acid alignment were treated as missing data, and phylogenetic information present in the gaps was then encoded as a binary dataset of the same length and analysed as the second partition. Each Metropolis-coupled Markov chain Monte Carlo (MCMC) run was three million generations long, sampled every 1000th step, and the first 30% of sampled trees were discarded as burn-in. The runs were considered converged when average standard deviation of split frequencies was less than 0.01 and potential scale reduction factor approached 1.0. The observed 95% confidence interval of the tree length did not include ML tree length estimate and branch lengths were subsequently calculated using ML approach on fixed BI tree topology in RAxML 7.2.6 [29]. The ML analysis was performed in PhyML 3.0 [30] with BIONJ selected as the starting tree and NNI tree topology search algorithm. Alignment gaps were treated as missing data and bootstrap support was estimated from 100 parametric replicates. Midpoint rooting was used in the analyses. Posterior probabilities ≥ 0.95 in BI analyses and bootstrap support ≥ 70% in ML analyses were designated significant. Analyses were conducted on computational clusters at the Institute of Vertebrate Biology AS CR, Brno, Czech Republic and Bioportal, University of Oslo, Norway.

3. Results

3.1. Sequence and phylogenetic analysis of pea aphid aquaporin genes

Detailed examination of the pea aphid genome [Acyr 2.0 primary assembly (NCBI)] resulted in the identification of three gene loci encoding proteins with aquaporin/MIP homology. The first locus corresponds to the aquaporin gene *ApAQP1* (ACYPI006387, Gene ID: 100165436 on scaffold NW_003383975). *ApAQP1* expression generates two isoforms by alternative splicing of the 5′ exons encoding proteins of 272 and 250 amino acids, respectively. The dominant isoform expressed in the gut is isoform-1 (272 amino acids, NP_001139376.1), which has been demonstrated previously to function as a Hg-sensitive water-selective aquaporin involved in water cycling and osmoregulation [9]. A second locus (Gene ID: 100573582, scaffold NW_003384268) encodes an aquaporin-like protein in which the amino-terminal 212 amino acids is identical to ApAQP1 isoform-1. However this protein diverges from the canonical aquaporin sequence with the 60 carboxyl terminal residues of ApAQP1 replaced by 41 amino acids that lack aquaporin/MIP pore forming determinants (the second NPA box and the LE_1 and LE_2 residues of the ar/R selectivity filter), suggesting that it is incapable of forming a functional aquaporin/MIP channel.

Another aquaporin-like gene (ACYPI009194, Gene ID: 100168499, scaffold NW_003383567), which we refer to as ApAQP2, encodes two transcriptional variants that encode separate protein isoforms: isoform-1 (308 amino acids [Fig. 1]) and isoform-2 (275 amino acids), which lacks the 33 N-terminal amino acids in isoform-1. Published EST data indicate that both isoforms of this gene are expressed in aphids [11]. This study focused on isoform-1, building on evidence that it is expressed in isolated bacteriocytes [12]. It contains all of the sequence and structural characteristics of the MIP channel family, including six predicted transmembrane domains and two canonical NPA boxes, all components of the prototypical “hourglass fold” of the aquaporin/MIP superfamily (Fig. 1).

The phylogenetic position of the ApAQP2 protein sequence was investigated by comparison with 60 animal MIP sequences using Bayesian (BI) and maximum likelihood (MI) methods. The tree topologies obtained with the two methods were very similar, assigning all but one of the sequences to one of four significantly supported clades, termed A–D (Fig. 2 shows the BI tree). Clade A contained a number of functionally characterized water-specific aquaporins from both mammals and insects. This clade contains the three insect subfamilies of aquaporins, BIBs, DRIPs, and PRIPs [2]. The previously characterized *A. pisum* aquaporin ApAQP1 [9] clusters within the PRIP subfamily. Clade C represents a group of functionally characterized mammalian-like aquaglyceroporins that includes AQP3, AQP7, and AQP9 [31–33]. Clade D MIPs are similar to human AQP11 and AQP12, which have been termed “superaquaporins”, and yet have poorly defined transport properties [34].

ApAQP2 was assigned to clade B, which differs from the other clades in that all members are of insect origin. Since ApAQP2 belongs to an insect-specific clade, distinct from other MIP family members with canonical aquaporin or aquaglyceroporin activities, structural and functional analyses were undertaken to model the putative transport pore and determine its transport selectivity.

3.2. Molecular modeling of ApAQP2

The structural properties of the putative transport pore of ApAQP2 were investigated by molecular modeling by using the Molecular Operating Environment (MOE) software. A homology model of the ApAQP2 protein was constructed utilizing the 1.8 Å X-ray structure (PDB ID 3GD8 [21]) of human AQP4 as a modeling template (Fig. 3).

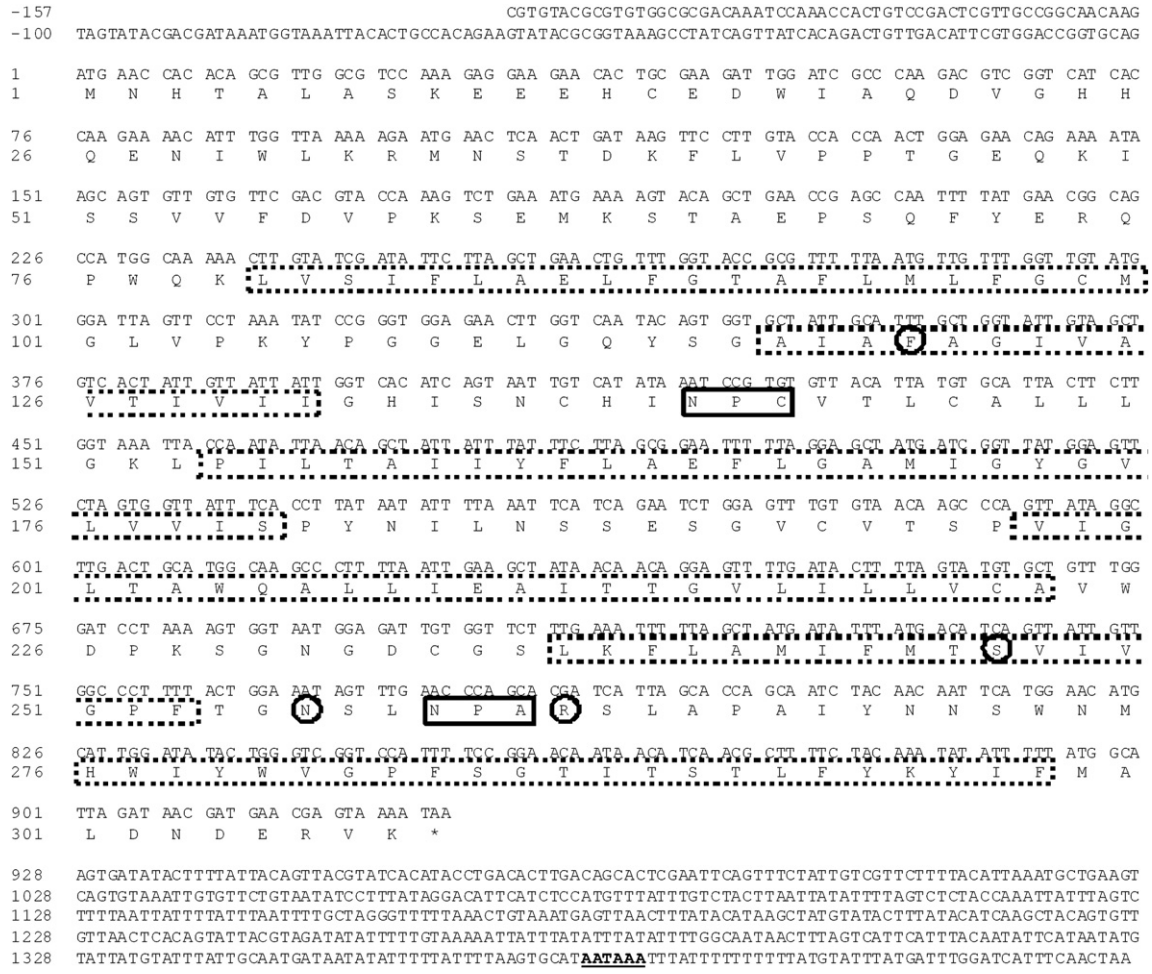

Fig. 1. Amino acid sequence of ApAQP2: The full length cDNA sequence of ApAQP2 showing the open reading frame and deduced amino acid sequence. The predicted transmembrane domains are highlighted in dashed boxes, the NPC and NPA motifs in solid boxes, and the residues of the proposed ar/R selectivity filter in solid circles. The position of a potential polyadenylation site in the 3′-untranslated region is underlined.

The structural alignment of the ApAQP2 homology model with the modeling template was excellent with an average carbon backbone root mean square deviation (rmsd) of 0.762 Å. All elements of the aquaporin fold were apparent which allowed modeling of the predicted pore determinant regions.

The selectivity-determining ar/R region consists of a tetrad of residues from transmembrane α-helices 2 (H2) and 5 (H5), as well as two residues from the 2nd NPA helical loop E (LE_1 and LE_2) [22]. In the human AQP4 X-ray structure, these residues are Phe 77, His 201, Ala 210, and Arg 216, respectively. This collection of ar/R residues, particularly a conserved His at the H5 position, is characteristic of water-selective aquaporins. In the AQP4 ar/R structure, water is bound by four hydrogen bonds collectively contributed by the sides chains of His 201, Arg 216, as well as by the backbone carbonyl of Ala210 [21]. These residues provide the necessary structural features to facilitate rapid water transport while the small ar/R diameter excludes larger solutes, resulting in a high conductance water-specific channel.

The ApAQP2 homology model suggests that the Phe residue at H2 and the Arg residue at LE_2 are conserved with respect to human AQP4 (Fig. 3B). Comparison of the predicted ar/R residues of Clade B MIPs suggests that these two aquaporin-like ar/R residues are conserved in other subfamily members as well (Table 1). However, ApAQP2 contains a Ser substitution at H5, which is a highly conserved His in AQP4 and other water-specific aquaporins. The presence of a Ser, Cys or Ala in the place of His is a characteristic feature of the Clade B insect MIPs (Table 1). At the LE_1 position, ApAQP2 possesses an unusual Asn residue, whereas water-selective aquaporins and other Clade B MIPs possess a smaller amino acid, typically Ala, Gly or Cys (Table 1). Modeling of the predicted ApAQP2 pore diameter using the HOLE program suggests that the ar/R region still forms a size constriction, albeit with a larger pore diameter compared to AQP4 (Fig. 3C). Overall, the novel ar/R region of ApAQP2 is atypical of water-specific aquaporins and mammalian aquaglyceroporins, suggesting that this protein may exhibit different functional properties and substrate selectivity compared to these well-characterized MIP channels.

3.3. Functional analysis of ApAQP2 transport

To investigate the functional properties of ApAQP2, the protein was expressed in *X. laevis* oocytes and subjected to water and solute transport analyses. Assays of ApAQP2-injected oocytes indicated that expression of this channel increases the osmotic water permeability (P_f) of the oocyte plasma membrane 15-fold, a clear indication of aquaporin activity (Fig. 4A). Western blot analysis confirmed that this increase in P_f corresponded with the expression of the ApAQP2 channel (Fig. 4B). The effect of $HgCl_2$, a classical aquaporin inhibitor, was also investigated. Unlike many aquaporins, including the water-selective ApAQP1 [9], the P_f of ApAQP2 oocytes treated with 1 mM $HgCl_2$ was not significantly different ($p = 0.265$) from untreated controls (Fig. 4C).

Due to the unusual composition of the ApAQP2 ar/R region, a broader range of test solutes was assayed to investigate the channel substrate selectivity. Similar to the well-characterized soybean

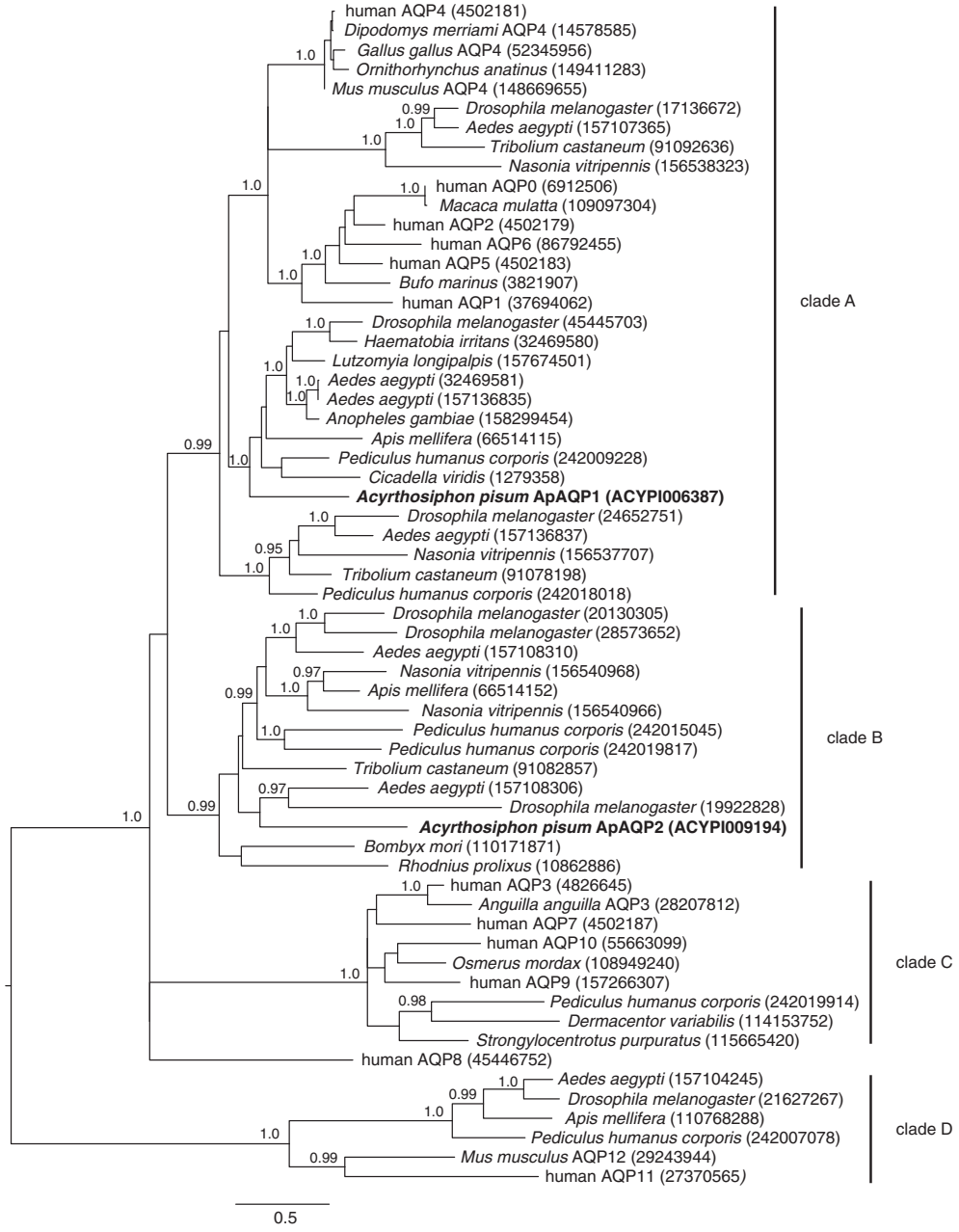

Fig. 2. Phylogenetic analysis of aphid aquaporins: A phylogenetic tree of animal aquaporin sequences was generated by Bayesian inference based on the Blosum62 rate matrix with gamma distribution of rate variation across sites. Numbers above edges denote statistically significant posterior probability (≥0.95). Genus and species names are indicated in italics with NCBI protein sequence identifiers indicated in parentheses. The sequences comprising the four phylogenetically supported clades (A–D) are labeled by vertical bars in the right margin. The sequence identifiers for ApAQP2, as well as the water-specific ApAQP1 [9] are shown in bold.

nodulin-26 aquaglyceroporin (GmNod26 in Table 1) [18,35], ApAQP2-expressing oocytes showed an increased permeability to ^{3}H-glycerol (Fig. 5A). However, ApAQP2-expressing oocytes also exhibited a 10-fold increase in permeability to the larger polyol mannitol, while the nodulin 26-expressing oocytes effectively excluded this solute (Fig. 5B).

Oocyte solute-dependent swelling assays were also performed to test ApAQP2 permeability to a wider range of polyols and model substrates. In agreement with the data from radioisotopic uptake assays, ApAQP2-expressing oocytes were permeable to mannitol as well as the epimeric six carbon alditols galacitol and sorbitol (Fig. 6). Additionally, ApAQP2-expressing oocytes were permeable to four carbon (erythritol) and five carbon (arabinitol, ribitol, xyltiol) alditols. The measured permeabilities for each solute were very similar, and the ApAQP2-expressing oocytes exhibited very little transport preference for alditol chain length or hydroxyl group stereochemistry. ApAQP2-expressing oocytes were also capable of transporting the uncharged test compounds formamide and urea, which are also common substrates for many aquaglyceroporins. However, ApAQP2-expressing oocytes were not permeable to the cyclic six-carbon polyol inositol. Overall, these results indicate a unusual substrate profile for ApAQP2 which forms a high-conductance, Hg-insensitive water channel that is also permeated by a broad but defined range of linear polyols.

3.4. Expression analysis of ApAQP2 in A. pisum

Previous studies have indicated that *ApAQP2* is expressed in whole aphid samples [11] and bacteriocytes [12]. To quantitate more precisely the expression pattern of *ApAQP2*, transcript levels in dissected pea aphid organs was investigated using real-time Q-PCR expression

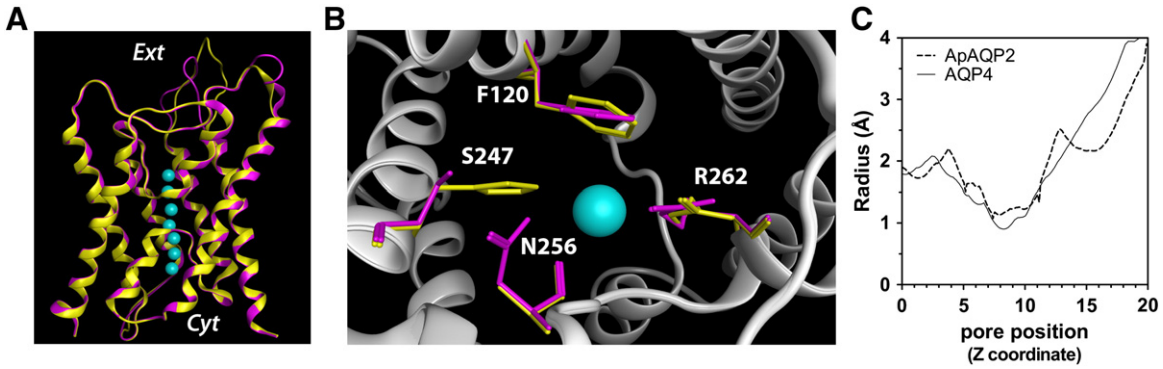

Fig. 3. Homology modeling analysis of ApAQP2 pore-forming residues: A homology model of ApAQP2 generated with the Molecular Operating Environment (MOE) software using the experimental AQP4 structure (pdb 3GD8) as a structural template. A. Superimposition of the structural model of ApAQP2 (fushia) and the AQP4 structure (yellow). The water molecules in the AQP4 pore are indicated by light blue spheres to show the position of the transport pore. The relative positions of the extracellular space (ex) and the cytosol (cyt) are indicated. B. The residues comprising the ar/R region of ApAQP2 (fushia) are shown viewed perpendicular to the transport pore axis from the extracellular face of the protein superimposed upon the corresponding residues in the AQP4 structure (yellow). Each ApAQP2 ar/R amino acid is labeled with the single letter amino acid designation as well as the residue index. The ar/R positions proceed counterclockwise as follows: H2, H5, LE_1, LE_2. The position of the transport substrate (water) bound to the ar/R region is indicated by the light blue sphere. C. Comparison of the ar/R regions of the AQP4 and ApAQP2 structures with HOLE. The calculated pore radius along the z-coordinate of the pore across the ar/R region is shown.

analysis (Fig. 7). ApAQP2 expression levels were significantly over-represented in the fat body (5.1-fold) and bacteriocytes (19.3-fold), and under-represented in the aphid gut.

Table 1
Conservation of pore-forming residues of insect clade B MIP sequences.

Protein[a]	Ar/R residues[b]				NPA motifs[c]	
	H2	H5	LE_1	LE_2	NPA1	NPA2
Selective aquaporins						
HsAQP4	F	H	A	R	NPA	NPA
ApAQP1	F	H	A	R	NPA	NPA
Aquaglyceroporins						
GmNod26	W	V	A	R	NPA	NPA
HsAQP3	F	G	Y	R	NPA	NPA
PfAQP	W	G	F	R	NLA	NPS
Glyceroporins						
EcGlpF	W	G	F	R	NPA	NPA
Clade B insect MIPs						
ApAQP2	F	S	N	R	NPC	NPA
AQP-Bom2	F	S	A	R	NPS	NPA
AaMIP1	F	A	A	R	NPA	NPA
AaMIP2	F	S	A	R	NPS	NPA
PhcMIP1	F	A	C	R	NPA	NPA
PhcMIP2	F	A	G	R	NPS	NPA
NvMIP1	F	A	C	R	NPA	NPV
NvMIP2	F	C	C	R	NPA	NPA
TcMIP	F	S	A	R	NPA	NTA
AmMIP	F	A	C	R	NPA	NPA
DmCG4019	F	A	G	R	NPA	NPA
DmCG17664	F	S	A	R	NPA	NPV
RpMIP	F	S	A	R	NPV	NPV

[a] The protein sequence name for each MIP isoform is indicated. Genus and species designations are as follows: Hs, *Homo sapiens*; Gm, *Glycine* max; Pf, *Plasmodium falciparum*; Ec, *Escherichia coli*; Ap, *Acrythosiphon pisum*; Rp, *Rhodnius prolixus*; Aa, *Aedes aegypti*;Phc, *Pediculus humanus corporis*; Nv, *Nassonia vitripennis*; Tc, *Tribolium castaneum*; Am, *Apis melifera*; Dm, *Drosophila melanogaster*. Accession number for these proteins are as follows: HsAQP4 (NP_001641), ApAQP1 (NP_001139376), GmNod26 (CAA28471), HsAQP3 (NP_004916), PfAQP (AAN35922); EcGlpF, (BAE77383); ApAQP2 (NP_001139377), AQP-Bom2 (BAE97427), AaMIP1 (XP_001650170), AaMIP2 (XP_001650168), PhcMIP1 (XP_002428189), PhcMIP2 (XP_002430355), NvMIP1 (XP_001601253), NvMIP2 (XP_001601231), TcMIP (XP_970728), AmMIP (XP_624194), DmCG4019 (NP_611813), DmCG17664 (NP_788433), and RpMIP (CAC13959).

[b] The residues comprising the helix 2 (H2), helix 5 (H5), loop E position 1 (LE_1) and loop E position 2 (LE_2) residues of the ar/R region are indicated for each sequence. A representative sequence alignment showing the position of each ar/R residue is shown in Supplementary Fig. 1.

[c] The residues comprising the N-terminal (NPA1) and C-terminal (NPA2) NPA motifs are shown for each sequence.

4. Discussion

This study has identified an aphid aquaglyceroporin gene, *ApAQP2*, that is preferentially expressed in the bacteriocytes and fat body of the pea aphid *Acyrthosiphon pisum*. *ApAQP2* is a member of an insect-specific clade (clade B MIPs) that is phylogenetically distinct from other known animal aquaporin and aquaglyceroporin sequences. In accordance with this observation, structural analysis of an ApAQP2 protein homology model indicates it contains novel substitutions within the proposed selectivity-determining ar/R region. Similar to water-selective aquaporins, Clade B MIPs contain a conserved Phe at the H2 position and the invariant Arg residue at the LE_2 position of the ar/R region. However, the Clade B ar/R possesses small neutral hydrophilic amino acids (Ser or Ala) at the H5 position that results in an overall wider and more hydrophilic selectivity filter compared to other insect and mammalian aquaporins (Table 1). ApAQP2 is unique among other clade B MIPs and most aquaporins since it contains an unusual Asn residue at the LE_1 position. This positions an additional side chain within the ar/R selectivity filter that could potentially create new hydrogen bonding contacts for transported solutes.

Functional analysis of ApAQP2 in *Xenopus* oocytes indicates that the protein possesses a multifunctional aquaglyceroporin activity capable of transporting both water and neutral polyol substrates. ApAQP2 is highly permeable to water, inducing a 15-fold increase in the P_f of the oolemma upon expression in *Xenopus* oocytes. However, unlike most aquaporins, including the water-selective aphid aquaporin ApAQP1 [9], ApAQP2 water permeability was not sensitive to the common aquaporin channel blocker $HgCl_2$. Although an unusual property, aquaporin channels that are insensitive to mercury ions have been documented [36,37]. The inability of Hg^{2+} to block these transporters could be the result of the absence a Cys residue near the transport pore.

While ApAQP2 transports glycerol in a manner similar to established animal (e.g., AQP3 [31]), higher plant (e.g., nodulin 26 [35]), protist (e.g., PfAQP [38]) and bacterial (e.g., GlpF [39]) aquaglyceroporins, it differs significantly from these proteins with regard to its polyol transport behavior. For example, the well characterized *E. coli* GlpF shows limited ability to transport longer polyol substrates. *E. coli* GlpF transports the five carbon polyol ribitol at a rate similar to the established biological substrate glycerol, but exhibits strong size and stereoselectivity preferences for other polyols, with epimers of ribitol (e.g., xylitol and arabinitol) showing low permeability, and the six carbon compounds mannitol and sorbitol showing complete impermeability [40]. Additionally, a multifunctional aquaglyceroporin isolated from *Plasmodium falciparum* (PfAQP) exhibited

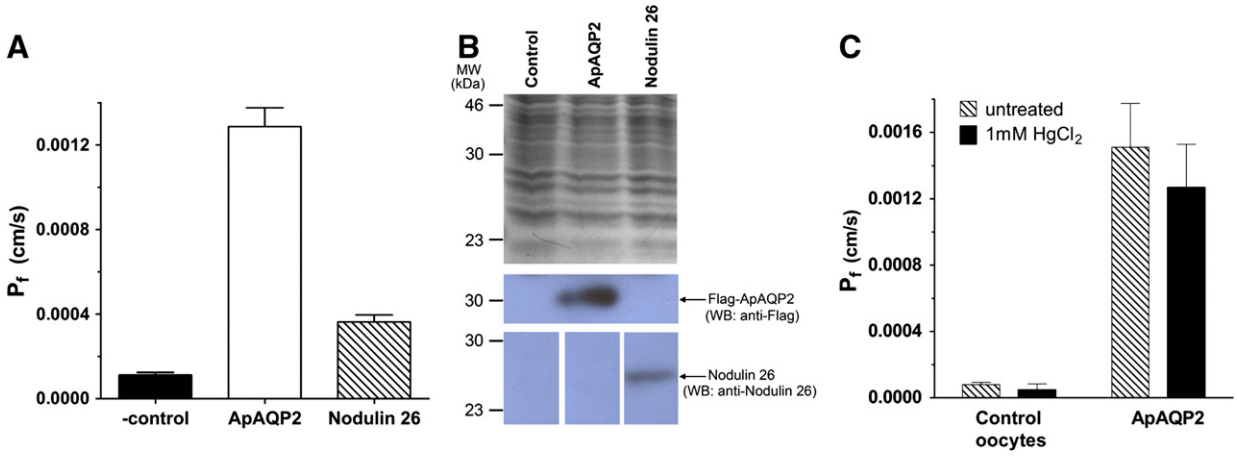

Fig. 4. Water permeability analysis of *Xenopus* oocytes expressing ApAQP2: A. *Xenopus* oocytes were injected 46 ng of *ApAQP2* cRNA (white bar) or soybean *nodulin 26* cRNA (hatched bar) and osmotic water permeability (P_f) was determined by the oocyte swelling assay. Oocytes injected with sterile RNase free-water were used as negative controls (black bar). Error bars represent SEM (n = 10 oocytes). B. Western blot analyses of oocyte lysates (20 μg total protein per lane). Top panel, Coomassie blue stained SDS-PAGE gel, middle panel, Western blot with anti-FLAG antibody, bottom panel, Western blot with anti-nodulin 26 antibody [55]. The positions of the molecular weight markers are indicated to the left of each panel. C. Negative control and ApAQP2-expressing oocytes were pre-treated with 1 mM $HgCl_2$ (solid black bars) prior to the standard water permeability assay described in Materials and methods. Untreated oocytes (hatched bars) were used as controls. Error bars represent SEM (n = 6–9 oocytes).

robust permeability to five carbon polyols with a preference for arabitol and xylitol. However, PfAQP was impermeable to the five carbon stereoisomer ribitol [38] and was also impermeable to the larger six carbon polyol mannitol [41]. In contrast, ApAQP2 shows strong permeability to a wide variety of linear polyols (C3 to C6) with little apparent preference for hydroxyl group stereochemistry, indicating a fundamental difference between in the transport pores of these classes of aquaglyceroporins.

Vertebrate aquaglyceroporins are a structurally and functionally conserved class of MIPs that cluster into a distinct phylogenetic group (Clade C) with a defined ar/R selectivity filter (Table 1). Interestingly, clade C MIPs are poorly represented in invertebrates whereas a diverse array of Clade B MIPs is represented in all insect species examined. This suggests that insects have acquired structurally and functionally distinct aquaglyceroporins compared to their vertebrate animal counterparts. It is unknown whether the broad array of polyol transport properties exhibited by ApAQP2 is shared by other clade B MIPs. Transport behavior of another clade B MIP, encoded by *AQP-Bom2* from the silkworm *Bombyx mori*, shows that it is able to transport water, glycerol and urea [42], but its selectivity and ability to transport larger polyols (e.g., mannitol or sorbitol) have not yet been assessed.

The variety of substrates transported by ApAQP2 also raises the question of the physiological function of water and polyol transport through this multifunctional channel. Based on Q-PCR expression analysis, *ApAQP2* is highly expressed in aphid bacteriocytes as well as in fat body cells. Both of these cell types are bathed in the hemolymph and actively engage in exchange of metabolites and solutes with this circulatory fluid. The osmotic pressure of the aphid hemolymph is tightly regulated within narrow limits, thereby protecting the fat body, bacteriocytes and other internal organs from the high and variable osmotic pressure of plant phloem sap ingested by the insect into the gut lumen [43,44]. One potential role for the robust aquaporin activity of ApAQP2 could be the maintenance of osmotic equilibrium between the hemolymph and bacteriocytes or fat body cells through rapid adjustments in water content.

With respect to aphid physiology, the polyol transport activity of ApAQP2 could also participate in carbohydrate metabolism and transport related to stress biology as well as the symbiosis with the *Buchera* bacteria. The accumulation of polyols including mannitol, sorbitol and erythritol in insects [45–47] has been linked to the ability of these compounds to protect proteins and membrane structures from denaturation and disruption in response to osmotic and temperature (cold or heat) stresses. In the case of aphids, both mannitol (*Aphis gossypii* [48]) and sorbitol (*Acyrthosiphon pisum* [49]) accumulate to high concentrations, particularly in response to heat stress, and may play a role in thermotolerance [49,50]. Polyols have been proposed to be synthesized from fructose precurors in the hemolymph via a ketone reductase activity isolated from whole aphids [50], although the discovery of a putative aldose reductase gene (ACYPI005685) expressed in the bacteriocytes and fat body ([51],

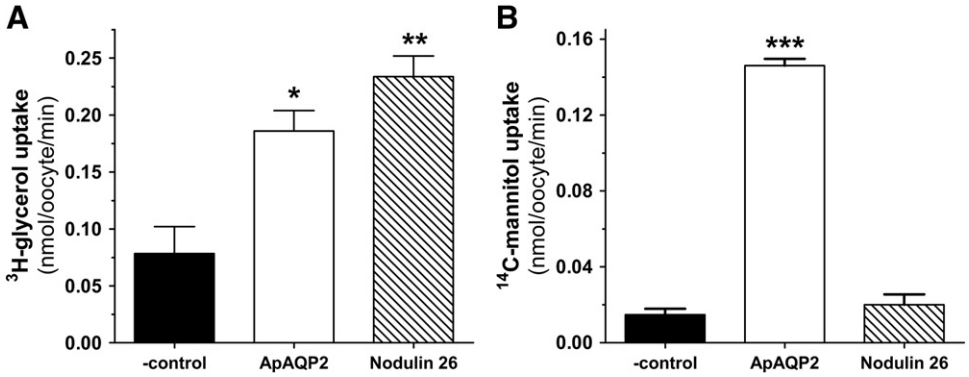

Fig. 5. Analysis of glycerol and mannitol permeabilities of ApAQP2 by radioisotopic substrate uptake: *Xenopus* oocytes injected with *ApAQP2* (white bars) or *nodulin-26* (hatched bars) cRNAs were assayed for uptake of A. ^{3}H-glycerol or B. ^{14}C-mannitol. Oocytes injected with sterile RNase-free water (black bars) were used as negative controls. Error bars represent SEM (n = 4). Asterisks over individual bars signify that transport rates are significantly higher than control oocytes (*p<0.05; **p<0.01; ***p<0.001).

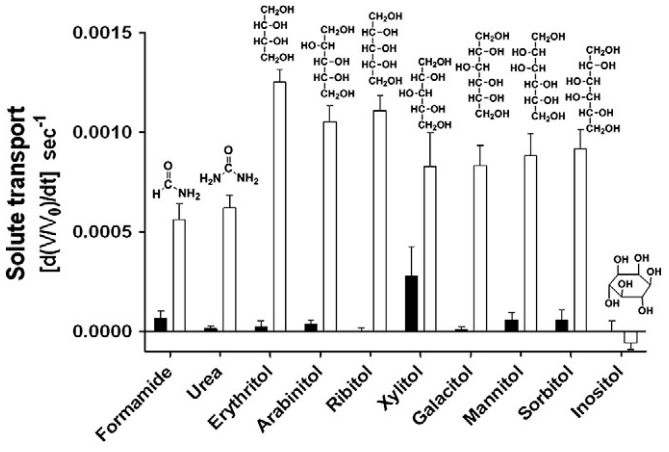

Fig. 6. ApAQP2 permeability to a series of polyol transport substrates: *Xenopus* oocytes were injected with *ApAQP2* cRNA, and were assayed for permeability to various solutes by video microscopy using an oocyte swelling assay (white bars). Oocytes injected with sterile RNase-free water (black bars) served as a negative control. Assays were conducted by immersion of oocytes in an isoosmotic Ringer's solution containing the test solutes shown above each bar. The swelling rates were measured as a change in oocyte volume [$(dV/V_0)/dt$] due to the uptake of each test solute followed by the osmotically-driven uptake of water. Error bars represent SEM (n = 10–24 oocytes).

Douglas, unpublished data) suggests additional potential sites of polyol biosynthesis. Since polyols are largely impermeable to lipid bilayers, the presence of a mannitol or a sorbitol facilitator such as ApAQP2 may be essential for the transport and partitioning of these critical protective polyols within bacteriocytes and fat body cells.

With respect to the bacteriocytes, ApAQP2 may have a symbiotic function. Most of the bacteriocyte cytoplasm is occupied by *Buchnera* cells, each of which is enclosed individually in a membrane of aphid origin ("the symbiosome membrane"). All metabolites required by the *Buchnera* and products of *Buchnera* metabolism are, of necessity, transported across the symbiosome membrane. The *Buchnera* genome is much reduced (0.64 Mb) and of small gene content (620 genes) [52], but it has retained the genes for a GlpF-like glycerol faciliator and a mannitol phosphotransferase system MtlAD, suggesting conservation of a polyol transport system. The potential significance of mannitol in the symbiosis is further underscored *in silico* analysis of the *Buchnera* metabolic network which suggests that it could represent an important carbon source for the endosymbiont [53,54]. In addition, the ability to take up and partition polyols between the aphid bacteriocyte cell cytosol, the internal space of the symbiosome, and *Buchnera* cells, may aid in osmoregulation. Based on the permeability profile of ApAQP2, and the observation that its expression is enriched in bacteriocytes, a potential transport function of these physiologically relevant polyols can be postulated. The determination of the ApAQP2 subcellular localization in bacteriocytes, including the determination of whether it is a symbiosome membrane protein, will provide valuable insight into these potential functions of this unusual aquaglyceroporin.

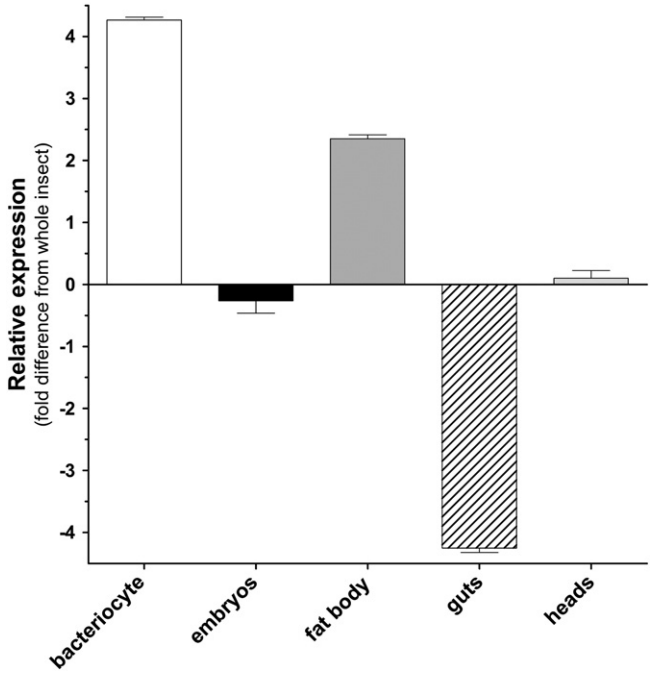

Fig. 7. Quantitative PCR analysis of *ApAQP2* gene expression in aphid tissues: Expression of the *ApAQP2* gene was normalized to the *RPL32* reference gene and standardized to the *ApAQP2* transcript expression level over the entire aphid body. Significant differences in expression (*) were determined by multiple t-tests with Bonferroni correction for five tests (critical probability $\alpha = 0.01$).

In summary, this study shows that the pea aphid aquaporin ApAQP2 is a multifunctional MIP that exhibits unprecedented substrate selectivity to both water and a wide range of potentially relevant linear polyols. Transport analyses suggest potential physiological functions of the protein in osmoregulation, as well as carbon nutrition of the insect and its symbiotic bacteria, and also provide a basis to investigate the transport properties of related MIPs in other insects. As a final note, it is also important to recognize that ApAQP2 is apparently expressed as two transcript variants that encode different protein isoforms that have the same core aquaporin-like pore structure but differ in the length of their cytosolic amino terminal regions. Further investigation is needed to determine the biological significance of these alternative splice variants in *Acyrthosiphon pisum* physiology.

Supplementary materials related to this article can be found online at doi:10.1016/j.bbamem.2011.11.032.

Acknowledgements

The authors acknowledge the assistance of Tian Li in the molecular modeling analyses. This study is supported in part by the National Science Foundation grant MCB-0618075, and a BBSRC Research Fellowship (BB/C520898) and the Sarkaria Institute of Insect Physiology and Toxicology.

References

[1] C. Hachez, F. Chaumont, Aquaporins: a family of highly regulated multifunctional channels, Adv. Exp. Med. Biol. 679 (2010) 1–17.
[2] E.M. Campbell, A. Ball, S. Hoppler, A.S. Bowman, Invertebrate aquaporins: a review, J. Comp. Physiol. B 178 (2008) 935–955.
[3] L.S. King, D. Kozono, P. Agre, From structure to disease: the evolving tale of aquaporin biology, Nat. Rev. Mol. Cell Biol. 5 (2004) 687–698.
[4] T. Walz, Y. Fujiyoshi, A. Engel, The AQP structure and functional implications, Handb. Exp. Pharmacol. 190 (2009) 31–56.
[5] B.L. de Groot, H. Grubmuller, Water permeation across biological membranes: mechanism and dynamics of aquaporin-1 and GlpF, Science 294 (2001) 2353–2357.
[6] L. Duchesne, J.F. Hubert, J.M. Verbavatz, D. Thomas, P.V. Pietrantonio, Mosquito (Aedes aegypti) aquaporin, present in tracheolar cells, transports water, not glycerol, and forms orthogonal arrays in Xenopus oocyte membranes, Eur. J. Biochem. 270 (2003) 422–429.
[7] M. Echevarria, R. Ramirez-Lorca, C.S. Hernandez, A. Gutierrez, S. Mendez-Ferrer, E. Gonzalez, J.J. Toledo-Aral, A.A. Ilundain, G. Whittembury, Identification of a new water channel (Rp-MIP) in the Malpighian tubules of the insect Rhodnius prolixus, Pflugers Arch. 442 (2001) 27–34.
[8] F. Le Caherec, S. Deschamps, C. Delamarche, I. Pellerin, G. Bonnec, M.T. Guillam, D. Thomas, J. Gouranton, J.F. Hubert, Molecular cloning and characterization of an insect aquaporin functional comparison with aquaporin 1, Eur. J. Biochem. 241 (1996) 707–715.
[9] A.J. Shakesby, I.S. Wallace, H.V. Isaacs, J. Pritchard, D.M. Roberts, A.E. Douglas, A water-specific aquaporin involved in aphid osmoregulation, Insect Biochem. Mol. 39 (2009) 1–10.
[10] I.A.G. Consortium, Genome sequence of the pea aphid Acyrthosiphon pisum, PLoS Biol. 8 (2010) e1000313.

[11] B. Sabater-Munoz, F. Legeai, C. Rispe, J. Bonhomme, P. Dearden, C. Dossat, A. Duclert, J.P. Gauthier, D.G. Ducray, W. Hunter, P. Dang, S. Kambhampati, D. Martinez-Torres, T. Cortes, A. Moya, A. Nakabachi, C. Philippe, N. Prunier-Leterme, Y. Rahbe, J.C. Simon, D.L. Stern, P. Wincker, D. Tagu, Large-scale gene discovery in the pea aphid Acyrthosiphon pisum (Hemiptera), Genome Biol. 7 (2006) R21.
[12] A. Nakabachi, S. Shigenobu, N. Sakazume, T. Shiraki, Y. Hayashizaki, P. Carninci, H. Ishikawa, T. Kudo, T. Fukatsu, Transcriptome analysis of the aphid bacteriocyte, the symbiotic host cell that harbors an endocellular mutualistic bacterium, Buchnera, Proc. Natl. Acad. Sci. U. S. A. 102 (2005) 5477–5482.
[13] A.E. Douglas, Phloem-sap feeding by animals: problems and solutions, J. Exp. Bot. 57 (2006) 747–754.
[14] E.A. Gunduz, A.E. Douglas, Symbiotic bacteria enable insect to use a nutritionally inadequate diet, P R Soc B 276 (2009) 987–991.
[15] N.A. Moran, J.P. McCutcheon, A. Nakabachi, Genomics and evolution of heritable bacterial symbionts, Annu. Rev. Genet. 42 (2008) 165–190.
[16] I.S. Wallace, D.M. Roberts, Distinct transport selectivity of two structural subclasses of the nodulin-like intrinsic protein family of plant aquaglyceroporin channels, Biochemistry 44 (2005) 16826–16834.
[17] J.F. Guenther, N. Chanmanivone, M.P. Galetovic, I.S. Wallace, J.A. Cobb, D.M. Roberts, Phosphorylation of soybean nodulin 26 on serine 262 enhances water permeability and is regulated developmentally and by osmotic signals, Plant Cell 15 (2003) 981–991.
[18] R.L. Rivers, R.M. Dean, G. Chandy, J.E. Hall, D.M. Roberts, M.L. Zeidel, Functional analysis of nodulin 26, an aquaporin in soybean root nodule symbiosomes, J. Biol. Chem. 272 (1997) 16256–16261.
[19] E.D. Vincill, K. Szczyglowski, D.M. Roberts, GmN70 and LjN70. Anion transporters of the symbiosome membrane of nodules with a transport preference for nitrate, Plant Physiol. 137 (2005) 1435–1444.
[20] N. Dascal, The use of Xenopus oocytes for the study of ion channels, CRC Crit. Rev. Biochem. 22 (1987) 317–387.
[21] J.D. Ho, R. Yeh, A. Sandstrom, I. Chorny, W.E. Harries, R.A. Robbins, L.J. Miercke, R.M. Stroud, Crystal structure of human aquaporin 4 at 1.8 A and its mechanism of conductance, Proc. Natl. Acad. Sci. U. S. A. 106 (2009) 7437–7442.
[22] I.S. Wallace, D.M. Roberts, Homology modeling of representative subfamilies of Arabidopsis major intrinsic proteins. Classification based on the aromatic/arginine selectivity filter, Plant Physiol. 135 (2004) 1059–1068.
[23] O.S. Smart, J.M. Goodfellow, B.A. Wallace, The pore dimensions of gramicidin A, Biophys. J. 65 (1993) 2455–2460.
[24] J.D. Thompson, T.J. Gibson, F. Plewniak, F. Jeanmougin, D.G. Higgins, The CLUSTAL_X windows interface: flexible strategies for multiple sequence alignment aided by quality analysis tools, Nucleic Acids Res. 25 (1997) 4876–4882.
[25] T.A. Hall, BioEdit: a user-friendly biological sequence alignment editor and analysis program for Windows 95/98/Nt, Nucleic Acids Symp. Ser. 41 (1999) 95–98.
[26] S. Whelan, N. Goldman, A general empirical model of protein evolution derived from multiple protein families using a maximum-likelihood approach, Mol. Biol. Evol. 18 (2001) 691–699.
[27] F. Abascal, R. Zardoya, D. Posada, ProtTest: selection of best-fit models of protein evolution, Bioinformatics 21 (2005) 2104–2105.
[28] F. Ronquist, J.P. Huelsenbeck, MrBayes 3: Bayesian phylogenetic inference under mixed models, Bioinformatics 19 (2003) 1572–1574.
[29] A. Stamatakis, RAxML-VI-HPC: maximum likelihood-based phylogenetic analyses with thousands of taxa and mixed models, Bioinformatics 22 (2006) 2688–2690.
[30] S. Guindon, O. Gascuel, A simple, fast, and accurate algorithm to estimate large phylogenies by maximum likelihood, Syst. Biol. 52 (2003) 696–704.
[31] M. Echevarria, E.E. Windhager, G. Frindt, Selectivity of the renal collecting duct water channel aquaporin-3, J. Biol. Chem. 271 (1996) 25079–25082.
[32] K. Ishibashi, M. Kuwahara, Y. Gu, Y. Tanaka, F. Marumo, S. Sasaki, Cloning and functional expression of a new aquaporin (AQP9) abundantly expressed in the peripheral leukocytes permeable to water and urea, but not to glycerol, Biochem. Biophys. Res. Commun. 244 (1998) 268–274.
[33] K. Ishibashi, M. Kuwahara, Y. Kageyama, A. Tohsaka, F. Marumo, S. Sasaki, Cloning and functional expression of a second new aquaporin abundantly expressed in testis, Biochem. Biophys. Res. Commun. 237 (1997) 714–718.
[34] K. Ishibashi, S. Hara, S. Kondo, Aquaporin water channels in mammals, Clin. Exp. Nephrol. 13 (2009) 107–117.
[35] R.M. Dean, R.L. Rivers, M.L. Zeidel, D.M. Roberts, Purification and functional reconstitution of soybean nodulin 26. An aquaporin with water and glycerol transport properties, Biochemistry 38 (1999) 347–353.
[36] M.J. Daniels, T.E. Mirkov, M.J. Chrispeels, The plasma membrane of Arabidopsis thaliana contains a mercury-insensitive aquaporin that is a homolog of the tonoplast water channel protein TIP, Plant Physiol. 106 (1994) 1325–1333.
[37] H. Hasegawa, T. Ma, W. Skach, M.A. Matthay, A.S. Verkman, Molecular cloning of a mercurial-insensitive water channel expressed in selected water-transporting tissues, J. Biol. Chem. 269 (1994) 5497–5500.
[38] E. Beitz, S. Pavlovic-Djuranovic, M. Yasui, P. Agre, J.E. Schultz, Molecular dissection of water and glycerol permeability of the aquaglyceroporin from Plasmodium falciparum by mutational analysis, Proc. Natl. Acad. Sci. U. S. A. 101 (2004) 1153–1158.
[39] C. Maurel, J. Reizer, J.I. Schroeder, M.J. Chrispeels, M.H. Saier Jr., Functional characterization of the Escherichia coli glycerol facilitator, GlpF, in Xenopus oocytes, J. Biol. Chem. 269 (1994) 11869–11872.
[40] D. Fu, A. Libson, L.J. Miercke, C. Weitzman, P. Nollert, J. Krucinski, R.M. Stroud, Structure of a glycerol-conducting channel and the basis for its selectivity, Science 290 (2000) 481–486.
[41] T. Zeuthen, B. Wu, S. Pavlovic-Djuranovic, L.M. Holm, N.L. Uzcategui, M. Duszenko, J.F. Kun, J.E. Schultz, E. Beitz, Ammonia permeability of the aquaglyceroporins from Plasmodium falciparum, Toxoplasma gondii and Trypansoma brucei, Mol. Microbiol. 61 (2006) 1598–1608.
[42] N. Kataoka, S. Miyake, M. Azuma, Aquaporin and aquaglyceroporin in silkworms, differently expressed in the hindgut and midgut of Bombyx mori, Insect Mol. Biol. 18 (2009) 303–314.
[43] A.E. Douglas, The nutritional physiology of aphids, Adv. Insect. Physiol. 31 (2003) 73–140.
[44] T.L. Wilkinson, D.A. Ashford, J. Pritchard, A.E. Douglas, Honeydew sugars and osmoregulation in the pea aphid Acyrthosiphon pisum, J. Exp. Biol. 200 (1997) 2137–2143.
[45] L. Lalouette, V. Kostal, H. Colinet, D. Gagneul, D. Renault, Cold exposure and associated metabolic changes in adult tropical beetles exposed to fluctuating thermal regimes, FEBS J. 274 (2007) 1759–1767.
[46] M.R. Michaud, J.B. Benoit, G. Lopez-Martinez, M.A. Elnitsky, R.E. Lee, D.L. Denlinger, Metabolomics reveals unique and shared metabolic changes in response to heat shock, freezing and desiccation in the Antarctic midge, Belgica antarctica, J. Insect Physiol. 54 (2008) 645–655.
[47] D. Doucet, V.K. Walker, W. Qin, The bugs that came in from the cold: molecular adaptations to low temperatures in insects, Cell. Mol. Life Sci. 66 (2009) 1404–1418.
[48] D.L. Hendrix, M.E. Salvucci, Polyol metabolism in homopterans at high temperatures: accumulation of mannitol in aphids (Aphididae: Homoptera) and sorbitol in whiteflies (Aleyrodidae: Homoptera), Comp. Biochem. Phys. A 120 (1998) 487–494.
[49] G. Burke, O. Fiehn, N. Moran, Effects of facultative symbionts and heat stress on the metabolome of pea aphids, ISME J. 4 (2010) 242–252.
[50] M.E. Salvucci, G.R. Wolfe, D.L. Hendrix, Purification and properties of an unusual NADPH-dependent ketose reductase from the silverleaf whitefly, Insect Biochem. Mol. 28 (1998) 357–363.
[51] A. Poliakov, C.W. Russell, L. Ponnala, H.J. Hoops, Q. Sun, A.E. Douglas, K.J. van Wijk, Large-scale label-free quantitative proteomics of the pea aphid-Buchnera symbiosis, Mol. Cell. Proteomics 10 (2011) M110.007039.
[52] S. Shigenobu, H. Watanabe, M. Hattori, Y. Sakaki, H. Ishikawa, Genome sequence of the endocellular bacterial symbiont of aphids Buchnera sp APS, Nature 407 (2000) 81–86.
[53] G.H. Thomas, J. Zucker, S.J. Macdonald, A. Sorokin, I. Goryanin, A.E. Douglas, A fragile metabolic network adapted for cooperation in the symbiotic bacterium Buchnera aphidicola, BMC Syst. Biol. 3 (2009).
[54] S.J. Macdonald, G.H. Thomas, A.E. Douglas, Genetic and metabolic determinants of nutritional phenotype in an insect-bacterial symbiosis, Mol. Ecol. 20 (2011) 2073–2084.
[55] Y. Zhang, D.M. Roberts, Expression of soybean nodulin 26 in transgenic tobacco. targeting to the vacuolar membrane and effects on floral and seed development, Mol. Biol. Cell 6 (1995) 109–117.